Published in final edited form as:
J Immunol. 2013 March 15; 190(6): 2736–2746. doi:10.4049/jimmunol.1201936.

Anti-IFNγ and peptide-tolerization therapies inhibit acute lung injury induced by crossreactive influenza-A (IAV)-specific memory T-cells

Myriam F. Wlodarczyk[*], **Anke R. Kraft**[*], **Hong D. Chen**[*], **Laurie L. Kenney**[*], and **Liisa K. Selin**[*]

[*]Department of Pathology and Program in Immunology and Virology, University of Massachusetts Medical School, Worcester, MA 01655;

Abstract

Viral infections have variable outcomes with severe disease occurring in only few individuals. We hypothesized that this variable outcome could correlate with the nature of responses made to previous microbes. To test this, mice were infected initially with IAV and in memory-phase challenged with LCMV, which we show here to have relatively minor cross-reactivity with IAV. The outcome in genetically identical mice varied from mild pneumonitis to severe acute lung injury with extensive pneumonia and bronchiolization, similar to that observed in patients that died of the 1918 H1N1 pandemic. Lesion expression did not correlate with virus titers. Instead, disease severity directly correlated with and was predicted by the frequency of IAV-$PB1_{703}$- and -PA_{224}-specific responses, which crossreacted with LCMV-GP_{34} and -GP_{276}, respectively. Eradication or functional ablation of these pathogenic memory T-cell populations, using mutant-viral strains, peptide-based tolerization strategies, or short-term anti-IFNγ treatment inhibited severe lesions such as bronchiolization from occurring. Heterologous immunity can shape outcome of infections and likely individual responses to vaccination, and can be manipulated to treat or prevent severe pathology.

Introduction

Typically the outcome of infections is quite variable between individuals. Reasons for such differences are multiple and the topic has been reviewed recently (1-5). We have championed the hypothesis that one relevant influence is the type of immune response made upon exposure to previous microbes. This heterologous immunity hypothesis was supported by observations in infectious mononucleosis where disease was more frequent in those showing crossreactive T-cell responses to a prior infection with influenza A (IAV)(6). Also, fulminant hepatitis induced by hepatitis C virus (HCV) is thought to occur more frequently in those individuals with a T-cell response that is narrowly focused on a crossreactive-epitope with IAV (7). We have developed mouse models of sequential unrelated viral infections to clarify the mechanisms of immunopathology. Specifically, we wanted to examine the development of severe acute lung injury during heterologous infections and to identify potential regimens to prevent this form of pathology.

More direct evidence for the relevance of heterologous immunity at influencing disease patterns during viral infections comes from studies in mice sequentially infected with two

Correspondence to Liisa K. Selin, Department of Pathology, Room S2-238, University of Massachusetts Medical School, 55 Lake Avenue North, Worcester, Massachusetts 01655, USA. Phone: (508) 856-3039; Fax: (508) 856-0019; liisa.selin@umassmed.edu.

Conflict of interest. The authors have no conflicting financial interests.

viruses. For instance, naive mice infected with vaccinia virus (VV) develop neutrophilic infiltrates and pulmonary edema (2, 3, 8), but lymphocytic choriomeningitis virus (LCMV)-immune mice infected with VV develop mononuclear infiltrates, associated with enhanced formation of complex lymph node-like structures known as bronchus-associated lymphoid tissue (BALT) (9, 10). Mice with more severe acute lung injury had necrotizing bronchiolitis, vasculitis and bronchiolitis obliterans (2), which in humans is a highly lethal pathology of unknown etiology associated with infections and transplant rejection (11, 12).

In the second mouse model, acute LCMV or murine cytomegalovirus infections result in mild interstitial mononuclear pneumonitis (3). However, IAV-immune mice infected with either virus could develop acute lung injury similar to that seen in individuals that died during the H1N1 IAV pandemic in 1918, with enhanced BALT, mononuclear pneumonia, necrotizing bronchiolitis, vasculitis and bronchiolization (13, 14). Bronchiolization, is an abnormal repair process where alveolar epithelium is replaced with bronchiolar-like epithelium, and in humans is considered pre-malignant and is associated with the development of the highly lethal condition, idiopathic pulmonary fibrosis (3, 15-17). However, the mechanisms involved in developing this severe lung pathology remain unknown. Here, we demonstrate that low frequency crossreactive IAV-specific CD8 memory T-cells were important in mediating severe lung injury in IAV-immune mice upon LCMV-infection and that this pathology was decreased by blocking the development or effector function of these crossreactive T-cells using either mutant-virus, peptide-based tolerization or anti-IFNγ-treatment.

METHODS

Virus infections of mice

6 wk old C57BL/6 male mice obtained from Jackson Laboratory (Bar Harbor,ME) after anesthetizing with metofane (Pitman-Moore, Mundelein,IL) were infected intranasally (*i.n.*) with 70 pfu of IAV-PR8 or PBS. After the immune system had returned to homeostasis (>6 wks), immune and control-mice were challenged *i.n.* with 1×10^5 pfu of LCMV(CL13 strain), which was propagated in baby hamster kidney (BHK21) cells. IAV-single-KO viruses PR-NP366, PR-PA224, and IAV-double-KO virus PR-NP366-PA224 were gifts from Drs. P.Thomas, S.Turner and R. Webby (18-21). These recombinant viruses were produced by using an established eight-plasmid reverse-genetics system (18-21). The PR plasmids have been described (19). Single amino acid mutations were introduced into the plasmids encoding the PRNP and PA genes by using PCR. Briefly, segment-specific fragments were amplified by using the universal primers described by Hoffman et al. (19) and internal primers designed with altered nucleotide sequences and terminal BsmB1 sites (New England Biolabs). These mutations resulted in the position-five asparagine of both epitopes being substituted for glutamine. The viruses with modified NP366 and PA224 segments are referred to as PR-NP and PR-PA, respectively (Supplemental figure 4). The double mutant is identified as PR-NP-PA. The LCMV-mutants (gift from Dr. M. Oldstone), NPV, GPV, and GP1V have single aa mutations in NP_{396}, both GP33/34 and GP_{276}, or $GP_{33/34}$ only, respectively (22, 23). The LCMV mutant viruses were generated by growing the virus in the presence of the various LCMV epitope-specific CD8 T cells resulting in epitope escape variants (Supplemental figure 4). In our experiments infection with any of the IAV- or LCMV-mutants resulted in similar virulence and morbidity as WT virus in normal B6 mice as has also been seen by others (Supplemental figure 4) (data not shown) (18-23). Age-matched immune and control-mice were housed in similar pathogen-free conditions for similar time-periods. This study was done in compliance within the guidelines of our IACUC.

Virus titration

LCMV titers were quantified in each organ (MLN, spleen and lung) by plaque assay using a 10% homogenate taken from individual mice, as described previously (5).

Synthetic peptides

Synthetic IAV-peptides $D^bPA_{224-233}$, $D^bNP_{366-374}$, and $K^bPB1_{703-711}$, LCMV-peptides D^bGP_{33-41}, $K^bGP_{34–41}$ and $D^bGP_{276–286}$ provided by Biosource International (Camarillo,CA) or 21st Century Biochemicals (Marlboro,MA) were used at 90% purity.

In vivo cytokine-depletion

IFNγ was depleted by injecting *i.v.* day D0 and D3, and daily *i.p.* 100μl rat anti-IFNγ (ATCC R4-6A2) ascites or control rat IgG-isotype (clone A110-1, Pharmingen, San Jose, CA) post infection (p.i.) with LCMV. TNF was depleted by injecting *i.p.* 100μg of TNFR2:IgG-Fc, (Etanercept; Immunex Corporation, Seattle WA) D-1 of LCMV-infection (24). Mip1-β or IL17 were depleted by injecting *i.p.* 100μg of either anti-Mip1-β (clone 46907; R&D Systems, Minneapolis MN) or anti-IL17 (clone 50104; R&D Systems) per mouse at D-1, 1, 2 and 4 of LCMV-infection (25). At D7.5 p.i. with LCMV lungs and spleens were collected for virus titrations and histological analysis.

Lung histological evaluation

D7.5 after LCMV challenge, lungs from IAV-immune and control-mice were collected, fixed in 10% neutral buffered formaldehyde and paraffin-embedded. Tissue sections (5 μm) were stained with hematoxylin and eosin (H&E) and analyzed microscopically. Scoring of lung pathology by a pathologist blinded to the experimental design was graded based on a previously described scale (3): 1: mild interstitial mononuclear infiltrates, disorganized BALT, perivascular edema. 2: moderate interstitial mononuclear infiltrates, small amount of organized BALT, pulmonary edema. 3: moderate interstitial mononuclear infiltrates, pulmonary edema, enhanced organized BALT, mild bronchiolization, mild consolidation. 4: severe interstitial mononuclear infiltrates, greatly enhanced pulmonary edema, enhanced organized BALT, moderate bronchiolization, moderate consolidation and moderate necrotizing bronchiolitis. 5: severe interstitial mononuclear infiltrates, greatly enhanced pulmonary edema, enhanced organized BALT, severe bronchiolization, severe consolidation, severe necrotizing bronchiolitis and vasculitis involving more than half of the lung. The scoring on each individual mouse was done on 4-5 different sections of the lung representing 4-5 different lobes of the whole lung assessing both qualitative and quantitative changes in histology (Supplemental figure 4). The histology photographs showing high power views of a small portion of one lobe of the lung demonstrate examples of the types of pathology observed in different treatment groups, but evaluations of the whole lung were used for scoring.

Cell lines

Splenocytes were isolated and plated at 7.5×10^5/ml together with peptide-pulsed (1μM), irradiated (30 Gy) TAP-2-deficient B6-derived T-lymphoma cell line, RMA cells, at 1.5×10^5/ml in 4 ml total volume per well of a 12-well plate. T-cell lines were fed with media (AIM-V [Gibco; Invitrogen corp., Carlsbad,CA.] supplemented with 20% FCS [Sigma Chemical Co., St. Louis,MO], 16% MLA-144 supernatant, 10 U/ml rIL-2 [BD], 1% l-glutamine [Gibco; Invitrogen corp., Carlsbad,CA.], 0.5% β-mercaptoethanol [Sigma-Aldrich, St Louis,MO], and 1% HEPES [Hyclone, Waltham, MA]) every 3-4 days and were restimulated with RMA cells weekly (26). After the first stimulation, the cells were plated at 2.5×10^5/ml together with peptide-pulsed (1μM), irradiated (30 Gy) RMA cells at 0.5×10^5/

ml in 4 ml total volume per well of a 12-well plate. After 3-4 wks of stimulation T-cell lines were analyzed.

Intracellular IFN-γ/TNF staining

LCMV or IAV-peptide-specific, IFNγ/TNF secreting CD8 T-cells were detected using Cytofix/Cytoperm kit (with GolgiPlug; BD Bioscience) as described previously (26) in combination with cell surface staining with CD8α(53-6.7), CD4 (GK1.5), CD44(IM7), IFN-γ(XMG1.2) and TNF(MP6-XT22) mAb purchased from BD Bioscience, San Jose, CA.

Cytokine-multiplex-assay

Splenocytes harvested D1, 3, 7, and 9 after LCMV-infection were lysed, and sent to Pierce/Searchlight (Rockford,IL) for Elisa Multiplex analysis of IFNγ.

Depletion of CD4 or CD8 virus-specific memory T-cells

3 wks after IAV or LCMV infection mice were injected *i.p.* on D0, 3, 7 and 10 with 100μg of either anti-CD8 (53-6.7) or - CD4 (GK1.5). Mice were then left to rest at least 3 wks to allow reconstitution of naïve T-cell pool.

Peptide-tolerization

Three wks after infecting 8 wk old mice with 70 pfu of IAV they were either injected *i.v.* with 250μg of PA_{224}, $PB1_{703}$, or NP_{366} peptide in PBS, or PBS following a previously established protocol to tolerize IAV-memory CD8 T-cells (27).

Elispot assay

PBMCs were prepared from blood and cells were plated in 96-well anti-IFNγ-coated plates (ebioscience, San Diego, CA), incubated 48h at 37°C, washed, and incubated with biotin-conjugated anti-IFNγ (ebioscience). Spots were visualized using biotin-conjugated peroxidase and read in a blinded fashion manually. In studies where the same individual mouse was followed sequentially, blood and spleen of IAV-immune mice, before or after LCMV-infection, respectively, were used (Supplemental figure 1).

Statistical analysis

Two-tailed Student's T tests were performed to compare two groups. Paired T-tests were used when following individual mice over time. Two-way ANOVA tests with Bonferroni post tests were used to compare more than two groups. Linear regression was used to measure correlation between two independent variables. Fisher's Exact test was used to measure differences between categorical data such as changes in immunodominant epitope or presence of bronchiolization. Statistical analysis was performed using GraphPad Prism Software. The data are expressed as means plus or minus SEM.

RESULTS

Memory CD8 T-cells in IAV-immune mice mediate severe lung pathology during subsequent LCMV-infection

Lung histology on day 7 of LCMV-infection of immunologically naïve mice revealed low levels of inflammation with mononuclear infiltration and mild pulmonary edema (Fig 1a.iii). In contrast, LCMV-infection of IAV-immune mice resulted in greatly increased lung pathology dominated by severe mononuclear pneumonic consolidation, enhanced BALT, necrotizing bronchiolitis, and bronchiolization, sometimes encompassing as much as half of the lung (Fig 1a.iv-vi). When the severity of lung pathology was scored based on the

magnitude and type of pathology present, IAV-immune mice had significantly greater pathology as compared to naïve mice at day 7 (Fig 1b) of LCMV-infection. Ultimately, both naïve and IAV-immune mice recovered from infection and resolved their acute lung injury.

Because the enhanced pathology resembled T-cell-dependent pathology, we hypothesized that memory T-cells generated during the first viral infection may have altered the pathology occurring after the second infection. In our experience, adoptively transferred memory T-cells effectively populate the spleen, but are poor at migrating into peripheral organs such as the lung, peritoneal cavity, or fat pads. Therefore, we developed an alternative new technique to preferentially deplete IAV-specific memory T-cells. Anti-CD4 or -CD8 mAb administered into IAV-immune mice resulted in depletion of these T-cell subsets. Thereafter, thymic emigrants renewed the naïve T-cell populations over the course of 3 wks, but there was a permanent loss of approximately 90% of IAV-specific memory CD8 T-cells (Supplemental figure 2a,b).

CD8- or CD4-depletion of naïve mice 4 wks prior to infection did not alter lung pathology **(Supplemental figure 2c,d)** or immune responses **(Supplemental figure 2f,g)** following acute infection with either LCMV or IAV, but, IAV-immune mice depleted of CD8 memory T-cells had significantly decreased lung pathology (Fig 1a.vii,c) as compared to non-depleted controls at day 7 of LCMV-infection (Fig 1a.iv,c). The lung histology in many of the memory CD8-depleted mice resembled that in naïve mice infected with LCMV (Fig 1a.iii), with mild mononuclear infiltrates. The vast majority of these memory CD8-depleted mice scored below level 3, when bronchiolization, the pathognomonic finding of severe pathology, is first observed (Supplemental figure 3). Although significantly decreased, the level of pathology in the CD8-depleted IAV-immune mice did not return to baseline levels observed in naïve mice upon LCMV-infection, perhaps because of the residual 10% of memory cells which were not depleted. Mice depleted of IAV-specific memory CD4 T-cells showed no decrease in lung pathology during LCMV-infection (Fig 1a.viii,cn). Thus, these results suggest that IAV-specific CD8, but not CD4 memory T-cells played a role in mediating severe lung pathology.

Viral load does not correlate with severity of lung pathology

IAV-immune mice infected with LCMV had significantly ($p<0.05$) increased LCMV titers in spleens (naïve+LCMV, 3.2±0.2 (SEM) pfu $\log_{10}$/ml; IAV+LCMV, 4.1±0.1, pfu $\log_{10}$/ml, n=5/gp) and lungs (naïve+LCMV, 4.6±0.1 pfu $\log_{10}$/ml; IAV+LCMV, 5.0±0.1 pfu $\log_{10}$/ml; n=5/gp). However, LCMV load in the lung or spleen did not correlate with the severity of lung pathology, suggesting that increased virus replication does not directly mediate lung pathology (Fig 1e). Furthermore, the severity of immunopathology did not increase in IAV-immune mice challenged with a 20-fold higher dose of LCMV (Fig 1d). Also, mice depleted of IAV-specific memory CD8 T-cells had similar LCMV titers as compared to control IAV-immune mice at day 7 of infection (IAV-control+LCMV, 4.2±0.1pfu $\log_{10}$/ml; IAV-CD8-depleted+LCMV, 4.2±0.2 pfu $\log_{10}$/ml; n=5/gp). Thus, these results suggest that IAV-specific memory CD8 T-cells rather than increasing viral load played a role in mediating increased lung pathology (Fig 1d,e).

Frequency of IAV-PA_{224} and -$PB1_{703}$-specific memory CD8 T-cells during LCMV-infection correlates with increased immunopathology

We hypothesized that memory CD8 T-cells that were crossreactive between the two viruses played a role in increasing immunopathology. A preferential expansion of a particular IAV-epitope-specific T-cell population in response to LCMV-infection would be suggestive of crossreactivity. By day 12 after LCMV-infection selective expansions of IAV-PA_{224}-(0.8%) or $PB1_{703}$-specific (0.63%) T-cells were found, as compared to their normal frequencies of

0.2% or .02%, respectively, observed in IAV-immune mice without LCMV-infection (Fig 2a,b). Individual IAV-immune mice expanded different T-cell responses during LCMV-infection, with IAV-$PB1_{703}$, -PA_{224}, or both T-cell memory responses becoming immunodominant in different individual mice (Supplemental figure 1g). In contrast, the normally immunodominant IAV-NP_{366} epitope-specific response did not increase or become immunodominant during LCMV-infection.

In the conventional prime(*i.p.*)/boost(*i.n*) IAV-infection mouse-model the IAV-NP_{366} response consistently dominates the acute immune response in the spleen of all mice (28). However, in our studies even before LCMV-infection, following the primary *i.n.* infection the IAV-immune immunodominance hierarchy varied greatly between individual mice, in that any of the 3 epitopes, $PB1_{703}$, NP_{366} and PA_{224}, could be dominant **(Supplemental figure 1e,f)**. In these IAV-immune control-mice NP_{366}-specific responses were most often the dominant response, while during LCMV-infection of IAV-immune mice $PB1_{703}$- and PA_{224}-specific responses were significantly more often dominant than NP_{366}-specific responses (Fig 2c, Supplemental figure 1).

To further control for this variation in immunodominance hierarchy between individual IAV-immune mice the same mouse was sequentially examined before and after LCMV-infection. Consistent with crossreactive expansion, there was a statistically significant proportional increase in $PB1_{703}$ (10/14 mice) and PA_{224} (7/14 mice) IAV-specific responses during LCMV-infection (Fig 2d). At the same time, NP_{366} (Fig 2e) or NS_2 (Fig 2f) showed either a significant proportional decrease or no change during LCMV-infection, consistent with these IAV-epitope-specific responses not being activated and therefore not crossreactive.

Furthermore, during LCMV-infection, the frequency of either PA_{224}- or $PB1_{703}$-specific memory T-cell responses directly correlated with the severity of lung pathology (Fig 2g,h), and the combined frequency of these two IAV-specific memory T-cell populations had an even stronger correlation (Fig 2i). In contrast, the frequency of the IAV-NP_{366}-specific memory T-cell response did not correlate with the intensity of lung pathology (Fig 2j). These results suggest that these low frequencies of IAV-PB1 and PA_{224}-specific memory cells were able to expand and induce severe lung pathology during LCMV-infection.

Decreased immunopathology upon elimination of crossreactive T-cell memory activation using IAV- or LCMV-epitope KO-viruses

In order to screen for the potential LCMV epitopes that were crossreactive with and stimulating the IAV-PB1 or -PA_{224} memory responses, we generated cell lines from IAV-immune mouse splenocytes, which had never been exposed to LCMV in vivo, by stimulating with LCMV peptides in vitro (Fig 3). These studies suggested 2 potential crossreactivities between IAV and LCMV epitopes. LCMV-GP_{276}(SGVENPGGYCL) was crossreactive to IAV-PA_{224}(SSLENFRAYV). These two H2-D^b-restricted epitopes have 40% sequence similarity (Fig 3d), so crossreactivity was not unexpected. The crossreactivity between H2-K^b-restricted LCMV-GP_{34}(AVYNFATC) and IAV-$PB1_{703}$(SSYRRPVGI) was unexpected, as there is little sequence similarity (Fig 3d). These crossreactivities may be weak, as LCMV peptides induced poor proliferation of the crossreactive population in these cell cultures from IAV-immune splenocytes (Fig 3a-f). Further, although functionally crossreactive as demonstrated by IFNγ production, these T-cells bound poorly to either tetramer. Also, although the IAV-PB1 or -PA_{224} specific T-cells expanded during the LCMV-infection in vivo (Fig 2), there was no clear evidence of the crossreactive LCMV-GP_{276} or -GP_{34}-specific populations dominating the LCMV response (data not shown).

Thus, to directly test if these crossreactive responses mediated the increased lung pathology, we used strains of IAV containing single amino acid mutations within the crossreactive IAV-PA_{224}, non-crossreactive IAV-NP_{366}, or both epitopes (18-21) (Supplemental figure 4i), which led to decreased antigen presentation and loss of these epitope-specific responses. Mice immunized with either PA_{224} or PA_{224}/NP_{336} mutant-viruses had significantly decreased lung pathology after LCMV challenge as compared to wt-IAV-immune controls (Fig 4a,b.iv). In agreement with the non-crossreactive nature of NP_{366} in this model system, mice immunized with the IAV-NP_{366}-mutant-virus did not show any decrease in lung pathology (Fig 4a,b.iii).

LCMV-variants that lacked the putative crossreactive-epitopes were also tested. We used LCMV-strains with single amino acid mutations in crossreactive-epitopes $GP_{33/34}$ and GP_{276} (LCMV-GPV), $GP_{33/34}$ (LCMV-GP1V), or non-crossreactive epitope NP_{396}, (LCMV-NPV), which led to dramatic decreases in these epitope-specific responses (22, 23) (Supplemental figure 4i). Only IAV-immune mice challenged with LCMV-mutants lacking $GP_{33/34}$ and GP_{276} together, or $GP_{33/34}$, showed significantly decreased lung pathology as compared to infection with wt-LCMV (Fig 4b.vi,c). IAV-immune mice challenged with either wt-LCMV or the NP_{396}-epitope mutant displayed lung pathology with similar degrees of severity (Fig 4b.v,c). These results are consistent with the hypothesis that memory IAV-PA_{224}-and -$PB1_{703}$-specific CD8 T-cells are likely crossreactive with LCMV-GP_{276} and -GP_{34}, respectively, and that these CD8 crossreactive T-cells were responsible for the severe acute lung injury during LCMV-infection.

Severe lung pathology can be predicted and prevented by epitope-specific tolerization of crossreactive memory T-cells

The severity of lung pathology varied between individual IAV-immune mice upon LCMV-infection (Fig 1), but this could be a reflection of the private specificity of T-cell responses within individual mice, as seen in other models of heterologous immunity (29, 30). Since *i.n.* infection with IAV led to variation between individual IAV-immune mice in the immunodominance hierarchy and level of memory responses to the 3 immunodominant epitopes (Supplemental figure 1e,f) (in contrast, to the prime/boost IAV-infection-model where NP_{336} responses dominate) (28) we questioned whether increased frequencies of the crossreactive memory populations would predict greater disease. There was a direct correlation between the size of the crossreactive IAV-$PB1_{703}$ and -PA_{224}, but not the non-crossreactive IAV-NP_{366} memory T-cell populations prior to LCMV-infection and the intensity of pathology after infection (Fig 5a,b). Thus, we could predict which IAV-immune mice were at greatest risk of developing severe immunopathology upon LCMV-infection.

We then tested whether functional inactivation of antigen-specific T-cells by peptide-tolerization, a technique successfully used in prevention of autoimmune diseases such as EAE (27, 31), would decrease pathology. We followed a method described by Linda Sherman's group to successfully tolerize IAV-specific memory T-cells in a manner which prevents the reactivation of these cells upon homologous IAV re-challenge (27). Mice were tolerized against IAV-epitope-specific responses by *i.v.* injection of the crossreactive peptides, $PB1_{703}$ and/or PA_{224}, or the non-crossreactive peptide, NP_{366} leading to an 80-90% reduction in these IAV-specific memory populations (Fig 6a,b). IAV-immune mice simultaneously tolerized with both crossreactive peptides (PA_{224} and $PB1_{703}$), showed significantly decreased severity of lung pathology (Fig 6d;e.vi) compared to IAV-immune mice **(Fig 6d;e.ii)**. In contrast, tolerization with either crossreactive peptide alone or the non-crossreactive NP_{366} peptide had no effect on decreasing pathology (Fig 6c;e.iii-v).

IFNγ blockade prevents pathology

We next questioned how crossreactive IAV-specific memory CD8 T-cells could potentially contribute to immunopathology and whether this knowledge could be used to develop other therapeutic interventions that would reduce disease severity. We did an initial screen for evidence of increases in inflammatory cytokines that activated memory CD8 T cells could produce in large amounts. ELISA-multiplex-analysis of total splenocyte lysates demonstrated that IAV-immune mice had significantly higher overall levels of IFNγ expression as compared to naïve mice during LCMV-infection **(Supplemental figure 3).** Other inflammatory cytokines that could be produced by activated T-cells, such as TNF, and Mip1β were not consistently expressed at higher levels (data not shown). Most importantly, IAV-immune mice treated with anti-IFNγ showed significantly decreased lung pathology compared to non-treated mice (Fig 7a,b). Blockade of IFNγ did not affect viral clearance (LCMV titers: spleen IAV+LCMV, 3.7±0.2 pfu $\log_{10}$/ml; IAV+α-IFNγ+LCMV, 3.6±0.3 pfu $\log_{10}$/ml; n=4/gp; lung IAV+LCMV, 5.0±0.2 pfu $\log_{10}$/ml; IAV+α-IFNγ+LCMV, 5.1±0.2 pfu $\log_{10}$/ml; n=4/gp) or significantly alter LCMV-specific T-cell responses (Fig 7c,d). This was consistent with studies showing a predominant role for perforin-mediated lysis (32, 33) and dispensable role for IFNγ (32) in CD8 T-cell control of LCMV-infection. Depletion of other cytokines that could potentially be produced by memory CD8 T-cells such as TNF, and Mip1β, did not significantly change peak immune responses or lung pathology upon LCMV-infection when compared with control IAV-immune mice (data not shown).

DISCUSSION

Experiments to date suggest that heterologous immunity may be a common phenomenon in human infections. Animal studies have indicated that most of the time it is beneficial, leading to protective immunity (2, 5, 34), but in some cases the wrong crossreactive response leads to a cascade of events that result in severe immunopathology (3, 4, 6, 7, 30). We are using mouse model systems to develop basic principles of heterologous immunity. This present study provides a formal demonstration that low frequencies of relatively weak CD8 T-cell crossreactivity between two unrelated viruses can be responsible for severe immunopathology. In our previous studies the crossreactive memory cells were at high frequencies, could be observed as double-tetramer reactive in vivo and caused dramatic skewing of the immunodominance hierarchies for both viruses(26, 29, 34, 35). This study was unique in that these crossreactive IAV-specific memory T-cells expanded, but remained at low frequencies, more analogous to human memory responses (6, 7). Further, they did not double-stain with tetramers directly ex vivo and did not alter the immunodominance hierarchy to the second virus.

We found a direct correlation between the frequency of crossreactive memory T-cell responses and the disease severity upon heterologous challenge and that mutation of these epitopes decreased the severity of acute lung injury. These results suggest that mapping crossreactive human T-cell epitopes could facilitate identification of individuals at heightened risk for developing severe lung injury during infection. Two therapeutic interventions, peptide-tolerization or short-term IFNγ-depletion, that functionally inhibited the effects of these crossreactive IAV-specific memory T-cells, were both effective at significantly decreasing lung pathology without affecting viral clearance. Thus, when more information about crossreactive-epitopes with pathogenic properties has accumulated, interventions by peptide-specific tolerization techniques may be of use to prevent severe disease in humans. More immediately, these studies suggest an awareness to eliminate deleterious crossreactive pathogenic epitopes from vaccines. This may reduce the generation

of memory T-cell populations with a potential for harmful pathological responses during subsequent infections.

This study indicates that immunotherapy to block IFNγ function short term may be useful for controlling severe acute lung injury during respiratory infections. IFNγ is important for clearance of some viruses (36), and is critically involved in activation of innate and adaptive immune responses. For instances, earlier studies suggested that IFNγ was not needed for T-cell expansion but was important for contraction of the response and thus memory responses were larger in IFNγ KO mice (37, 38). However, subsequently this was challenged by Dr. Lindsay Whitton and his colleagues (39, 40), who suggested that persisting virus in IFNγ KO mice might prevent appropriate T-cell contraction. They further demonstrated that IFNγR KO T-cells do not compete as well during a LCMV infection as wild type T-cells and that memory may be qualitatively different. These studies were done in the complete absence of IFNγ.

However, excessive or dysregulated IFNγ responses can lead to increased pathology (1-3, 5, 41, 42). IFNγ is a key contributor to human pulmonary injury and to the viral-storm during SARS infection and in acute respiratory distress syndrome (43-45). At this time we do not know if the increased IFNγ levels were produced directly by the activation of the cross-reactive memory T-cells or by other immune cells that the crossreactive T-cells activate. It is also not clear how IFNγ contributes to increasing lung pathology other than that IFNγ is a potent immuno-stimulatory cytokine that further amplifies both APC, macrophage and T-cell activity and in excess would create an over-activated immune environment, that may be difficult to shut down. However, by temporarily reducing the overall IFNγ production or by tolerizing crossreactive memory cells that may be producing or amplifying IFNγ production during the heterologous infection with LCMV, we attenuated the immunopathology. Fortunately, this temporary and most likely only partial depletion of excessive IFNγ had no effect on the generation of normal CD8 T-cell responses during the LCMV infection. Many human viruses, such as SARS, EBV, varicella-zoster and the 1918 or 2010 H1N1 IAV-strains (which can result in lung pathology similar to our heterologous infection mouse model) (13, 14), cause much more severe disease in young healthy adults, who have large complex memory populations, than in young children (46-48). Short-term appropriately timed anti-IFNγ-treatment, which is available (49, 50), may be useful in these kinds of circumstances.

Supplementary Material

Refer to Web version on PubMed Central for supplementary material.

Acknowledgments

We thank N. Aslan, P. Durost, S. Nie for expert assistance and A. Peixoto, S. Waggoner, and R. Welsh for critical review of the manuscript. The contents of this publication are solely the responsibility of the authors and do not represent the official view of the NIH.

Funding: This study was supported by NIH grant AI-46578 (LKS), AI-46629 (LKS), DK-32520 and T32 AI-07349-16 (LLK).

Nonstandard Abbreviations used

LCMV	lymphocytic choriomeningitis virus
IAV	influenza-A virus
TCR	T-cell receptor

IFN	interferon
TNF	tumor necrosis factor
BALT	bronchus-associated lymphoid tissue
VV	vaccinia virus
AFN	acute fatty necrosis
KO	knock out
aa	amino acid
IM	acute infectious mononucleosis
p.i.	post infection
XR	crossreactive

References

1. Rouse BT, Sehrawat S. Immunity and immunopathology to viruses: what decides the outcome? Nat Rev Immunol. 10:514–526. [PubMed: 20577268]
2. Chen HD, Fraire AE, Joris I, Brehm MA, Welsh RM, Selin LK. Memory CD8+ T cells in heterologous antiviral immunity and immunopathology in the lung. Nature immunology. 2001; 2:1067–1076. [PubMed: 11668342]
3. Chen HD, Fraire AE, Joris I, Welsh RM, Selin LK. Specific history of heterologous virus infections determines anti-viral immunity and immunopathology in the lung. The American journal of pathology. 2003; 163:1341–1355. [PubMed: 14507643]
4. Welsh RM, Selin LK. No one is naive: the significance of heterologous T-cell immunity. Nat Rev Immunol. 2002; 2:417–426. [PubMed: 12093008]
5. Selin LK, Varga SM, Wong IC, Welsh RM. Protective heterologous antiviral immunity and enhanced immunopathogenesis mediated by memory T cell populations. J Exp Med. 1998; 188:1705–1715. [PubMed: 9802982]
6. Clute SC, Watkin LB, Cornberg M, Naumov YN, Sullivan JL, Luzuriaga K, Welsh RM, Selin LK. Cross-reactive influenza virus-specific CD8+ T cells contribute to lymphoproliferation in Epstein-Barr virus-associated infectious mononucleosis. J Clin Invest. 2005; 115:3602–3612. [PubMed: 16308574]
7. Urbani S, Amadei B, Fisicaro P, Pilli M, Missale G, Bertoletti A, Ferrari C. Heterologous T cell immunity in severe hepatitis C virus infection. J Exp Med. 2005; 201:675–680. [PubMed: 15753202]
8. Galani V, Tatsaki E, Bai M, Kitsoulis P, Lekka M, Nakos G, Kanavaros P. The role of apoptosis in the pathophysiology of Acute Respiratory Distress Syndrome (ARDS): an up-to-date cell-specific review. Pathol Res Pract. 206:145–150. [PubMed: 20097014]
9. Tschernig T, Pabst R. Bronchus-associated lymphoid tissue (BALT) is not present in the normal adult lung but in different diseases. Pathobiology. 2000; 68:1–8. [PubMed: 10859525]
10. Moyron-Quiroz JE, Rangel-Moreno J, Kusser K, Hartson L, Sprague F, Goodrich S, Woodland DL, Lund FE, Randall TD. Role of inducible bronchus associated lymphoid tissue (iBALT) in respiratory immunity. Nat Med. 2004; 10:927–934. [PubMed: 15311275]
11. Selin LK, Brehm MA. Frontiers in nephrology: heterologous immunity, T cell cross-reactivity, and alloreactivity. J Am Soc Nephrol. 2007; 18:2268–2277. [PubMed: 17634431]
12. Schlesinger C, Meyer CA, Veeraraghavan S, Koss MN. Constrictive (obliterative) bronchiolitis: diagnosis, etiology, and a critical review of the literature. Ann Diagn Pathol. 1998; 2:321–334. [PubMed: 9845757]
13. Kuiken T, Taubenberger JK. Pathology of human influenza revisited. Vaccine. 2008; 26(Suppl 4):D59–66. [PubMed: 19230162]

14. Taubenberger JK, Morens DM. The pathology of influenza virus infections. Annual review of pathology. 2008; 3:499–522.
15. Nettesheim P, Szakal AK. Morphogenesis of alveolar bronchiolization. Lab Invest. 1972; 26:210–219. [PubMed: 5059985]
16. Minagawa S, Araya J, Numata T, Nojiri S, Hara H, Yumino Y, Kawaishi M, Odaka M, Morikawa T, Nishimura SL, Nakayama K, Kuwano K. Accelerated epithelial cell senescence in IPF and the inhibitory role of SIRT6 in TGF-beta-induced senescence of human bronchial epithelial cells. Am J Physiol Lung Cell Mol Physiol. 2011; 300:L391–401. [PubMed: 21224216]
17. Chilosi M, Poletti V, Zamo A, Lestani M, Montagna L, Piccoli P, Pedron S, Bertaso M, Scarpa A, Murer B, Cancellieri A, Maestro R, Semenzato G, Doglioni C. Aberrant Wnt/beta-catenin pathway activation in idiopathic pulmonary fibrosis. The American journal of pathology. 2003; 162:1495–1502. [PubMed: 12707032]
18. Andreansky SS, Stambas J, Thomas PG, Xie W, Webby RJ, Doherty PC. Consequences of immunodominant epitope deletion for minor influenza virus-specific CD8+-T-cell responses. Journal of virology. 2005; 79:4329–4339. [PubMed: 15767433]
19. Hoffmann E, Krauss S, Perez D, Webby R, Webster RG. Eight-plasmid system for rapid generation of influenza virus vaccines. Vaccine. 2002; 20:3165–3170. [PubMed: 12163268]
20. Thomas PG, Brown SA, Keating R, Yue W, Morris MY, So J, Webby RJ, Doherty PC. Hidden epitopes emerge in secondary influenza virus-specific CD8+ T cell responses. J Immunol. 2007; 178:3091–3098. [PubMed: 17312156]
21. Webby RJ, Andreansky S, Stambas J, Rehg JE, Webster RG, Doherty PC, Turner SJ. Protection and compensation in the influenza virus-specific CD8+ T cell response. Proc Natl Acad Sci USA. 2003; 100:7235–7240. [PubMed: 12775762]
22. Lewicki HA, Von Herrath MG, Evans CF, Whitton JL, Oldstone MB. CTL escape viral variants. II. Biologic activity in vivo. Virology. 1995; 211:443–450. [PubMed: 7645248]
23. Oldstone MB, Lewicki H, Borrow P, Hudrisier D, Gairin JE. Discriminated selection among viral peptides with the appropriate anchor residues: implications for the size of the cytotoxic T-lymphocyte repertoire and control of viral infection. Journal of virology. 1995; 69:7423–7429. [PubMed: 7494247]
24. Nie S, Cornberg M, Selin LK. Resistance to vaccinia virus is less dependent on TNF under conditions of heterologous immunity. J Immunol. 2009; 183:6554–6560. [PubMed: 19846867]
25. Hamada H, Garcia-Hernandez Mde L, Reome JB, Misra SK, Strutt TM, McKinstry KK, Cooper AM, Swain SL, Dutton RW. Tc17, a unique subset of CD8 T cells that can protect against lethal influenza challenge. J Immunol. 2009; 182:3469–3481. [PubMed: 19265125]
26. Cornberg M, Chen AT, Wilkinson LA, Brehm MA, Kim S-K, Calcagno C, Ghersi D, Puzone R, Celada F, Welsh RM, Selin LK. Narrowed TCR repertoire and viral escape as a consequence of heterologous immunity. J Clin Invest. 2006; 116:1443–1456. [PubMed: 16614754]
27. Kreuwel HTC, Aung S, Silao C, Sherman LA. Memory CD8(+) T cells undergo peripheral tolerance. Immunity. 2002; 17:73–81. [PubMed: 12150893]
28. Belz GT, Xie W, Doherty PC. Diversity of epitope and cytokine profiles for primary and secondary influenza a virus-specific CD8+ T cell responses. J Immunol. 2001; 166:4627–4633. [PubMed: 11254721]
29. Kim S-K, Cornberg M, Wang XZ, Chen HD, Selin LK, Welsh RM. Private specificities of CD8 T cell responses control patterns of heterologous immunity. J Exp Med. 2005; 201:523–533. [PubMed: 15710651]
30. Nie S, Lin S.-j. Kim S-K, welsh RM, Selin LK. Pathological features of heterologous immunity are regulated by the private specificties of the immune repertoire. Am J. Path. 2010; 176:2107–2112. [PubMed: 20348239]
31. Kyburz D, Aichele P, Speiser DE, Hengartner H, Zinkernagel RM, Pircher H. T cell immunity after a viral infection versus T cell tolerance induced by soluble viral peptides. Eur J Immunol. 1993; 23:1956–1962. [PubMed: 8344359]
32. Badovinac VP, Hamilton SE, Harty JT. Viral infection results in massive CD8+ T cell expansion and mortality in vaccinated perforin-deficient mice. Immunity. 2003; 18:463–474. [PubMed: 12705850]

33. Rode M, Balkow S, Sobek V, Brehm R, Martin P, Kersten A, Dumrese T, Stehle T, Müllbacher A, Wallich R, Simon MM. Perforin and Fas act together in the induction of apoptosis, and both are critical in the clearance of lymphocytic choriomeningitis virus infection. Journal of virology. 2004; 78:12395–12405. [PubMed: 15507626]
34. Cornberg M, Clute SC, Watkin LB, Saccoccio FM, Kim SK, Naumov YN, Brehm MA, Aslan N, Welsh RM, Selin LK. CD8 T cell cross-reactivity networks mediate heterologous immunity in human EBV and murine vaccinia virus infections. J Immunol. 2010; 184:2825–2838. [PubMed: 20164414]
35. Brehm MA, Pinto AK, Daniels KA, Schneck JP, Welsh RM, Selin LK. T cell immunodominance and maintenance of memory regulated by unexpectedly cross-reactive pathogens. Nature immunology. 2002; 3:627–634. [PubMed: 12055626]
36. Müller U, Steinhoff U, Reis LF, Hemmi S, Pavlovic J, Zinkernagel RM, Aguet M. Functional role of type I and type II interferons in antiviral defense. Science. 1994; 264:1918–1921. [PubMed: 8009221]
37. Harty JT, Badovinac VP. Influence of effector molecules on the CD8(+) T cell response to infection. Current opinion in immunology. 2002; 14:360–365. [PubMed: 11973135]
38. Lohman BL, Welsh RM. Apoptotic regulation of T cells and absence of immune deficiency in virus-infected gamma interferon receptor knockout mice. Journal of virology. 1998; 72:7815–7821. [PubMed: 9733817]
39. Whitmire JK, Benning N, Eam B, Whitton JL. Increasing the CD4+ T cell precursor frequency leads to competition for IFN-gamma thereby degrading memory cell quantity and quality. J Immunol. 2008; 180:6777–6785. [PubMed: 18453598]
40. Whitmire JK, Eam B, Benning N, Whitton JL. Direct interferon-gamma signaling dramatically enhances CD4+ and CD8+ T cell memory. J Immunol. 2007; 179:1190–1197. [PubMed: 17617612]
41. Bruder D, Srikiatkhachorn A, Enelow RI. Cellular immunity and lung injury in respiratory virus infection. Viral Immunol. 2006; 19:147–155. [PubMed: 16817757]
42. Baccala R, Kono DH, Theofilopoulos AN. Interferons as pathogenic effectors in autoimmunity. Immunol Rev. 2005; 204:9–26. [PubMed: 15790347]
43. Huang KJ, Su IJ, Theron M, Wu YC, Lai SK, Liu CC, Lei HY. An interferon-gamma-related cytokine storm in SARS patients. Journal of medical virology. 2005; 75:185–194. [PubMed: 15602737]
44. Theron M, Huang KJ, Chen YW, Liu CC, Lei HY. A probable role for IFN-gamma in the development of a lung immunopathology in SARS. Cytokine. 2005; 32:30–38. [PubMed: 16129616]
45. Wong CK, Lam CW, Wu AK, Ip WK, Lee NL, Chan IH, Lit LC, Hui DS, Chan MH, Chung SS, Sung JJ. Plasma inflammatory cytokines and chemokines in severe acute respiratory syndrome. Clinical and experimental immunology. 2004; 136:95–103. [PubMed: 15030519]
46. Simonsen L, Clarke MJ, Schonberger LB, Arden NH, Cox NJ, Fukuda K. Pandemic versus epidemic influenza mortality: a pattern of changing age distribution. The Journal of infectious diseases. 1998; 178:53–60. [PubMed: 9652423]
47. Weinstein L, Meade RH. Respiratory manifestations of chicken pox; special consideration of the features of primary varicella pneumonia. AMA Arch Intern Med. 1956; 98:91–99. [PubMed: 13338899]
48. Rickinson, ABK.; E.. Virology. Lippincott-Raven; Philadelphia: 1996.
49. Cottone M, Orlando A, Renna S. Investigational agents for Crohn's disease. Expert Opin Investig Drugs. Oct; 2010 19(10):1147–1159.
50. Skurkovich S, Kasparov A, Narbut N, Skurkovich B. Treatment of corneal transplant rejection in humans with anti-interferon-gamma antibodies. Am J Ophthalmol. 2002; 133:829–830. [PubMed: 12036679]

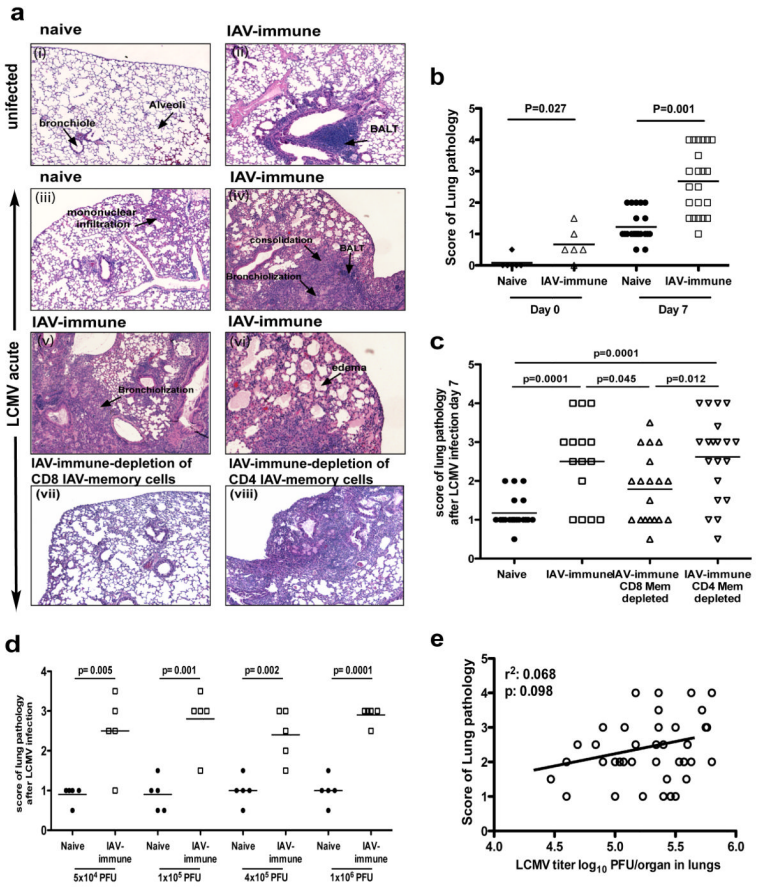

Figure 1. Memory CD8 T-cells but not viral load in IAV-immune mice directly mediate increased lung pathology during LCMV-infection

CD8 memory T-cells were depleted in IAV-immune mice by *i.p.* injection of anti-CD8 or -CD4 every 3 days for 3 doses. Mice were rested for 3-4 wks to allow reconstitution of the naïve cell pool. **(a)** Lung sections from naïve (**i**), IAV-immune (**ii**), 7 days p.i. with LCMV (**iii**), IAV-immune 7 days p.i. with LCMV (**iv-vi**) with CD8-depletion **(vii)** or CD4-depletion **(viii)** mice were stained with H&E. Photographs depict a representative section showing a high power view of a small part of one of the 4-5 different lung sections that were used for scoring in each individual mouse demonstrating the type of lung pathology observed in each group. (**i**) Naïve mice showed normal lung architecture. (**ii**) IAV-immune mice showed normal lung structure with some residual BALT. (**iii**) LCMV-infected control-mice showed mild lymphocytic interstitial infiltrates and mild BALT. (**iv-vi**) IAV+LCMV mice showed greatly increased BALT, edema, bronchiolization, consolidation and necrotizing bronchiolitis, which was diminished with CD8 (**vii**) but not CD4 (**viii**) depletion. (**b,c**) Lung pathology was scored and the data was pooled from 4 expts (n=3-5 mice/gp/expt). **(d,e)** There was no correlation between severity of lung pathology and splenic LCMV titers in the same mouse at day 7 p.i. in IAV-immune or naïve mice. **(d)** Lung sections from naïve **(full circle)** or IAV-immune mice **(open square)** 7 days p.i. with different doses of LCMV were stained with H&E and scored. Data were pooled from 4 experiments (n=3-5 mice/gp/expt) **(e)** Lungs from naïve or IAV-immune mice day 7 LCMV-infection, were stained with H&E and plaque for virus. Pathology was scored. The data were pooled from 5 expts (n=3-5 mice/gp/expt).

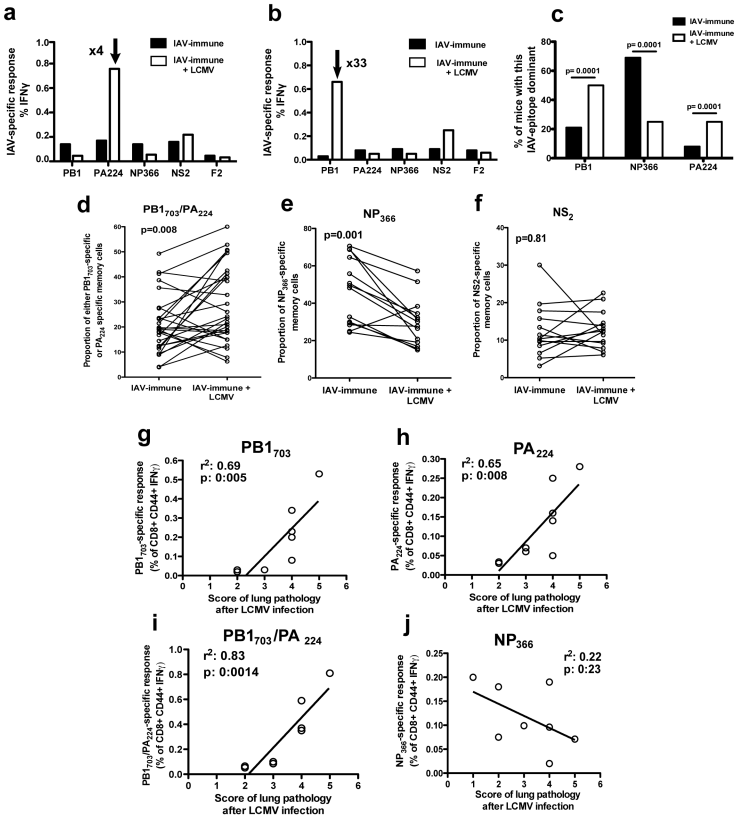

Figure 2. Direct correlation between severity of lung pathology and frequency of IAV-specific memory T-cells during LCMV-infection

(**a,b**) Splenocytes were harvested from IAV-immune mice day 7 p.i. with LCMV. Hierarchy of the IAV-specific memory response was determined by IFN**γ** production before (☐) and after LCMV-infection (☐) in separate mouse. Data are representative of individual mice in 2 experiments. **(c)** The percentage of mice using a particular IAV epitope as the dominant response before (n=12) and after LCMV (n=20) infection was calculated. Statistical test was Fischer's Exact test. (**d-f**) Proportional IAV-epitope-specific memory responses were calculated from IFN**γ** production assays using elispot in the blood before or ICS in the spleen after LCMV-infection of IAV-immune mice. Blood and spleen have similar immunodominance hierarchies in the same mouse (Supplemental figure 1). Paired Student's T test was used in d-f. (**g-j)** Lung pathology was scored. At the same time $PB1_{703}$, PA_{224} and NP_{366} IAV-specific memory responses were measured by IFN**γ**/TNF production. The relationship between the intensity of lung pathology and the frequency of IAV-specific memory T-cells was evaluated by linear regression. Data were pooled from 3 experiments (n=2-4 mice/gp/expt).

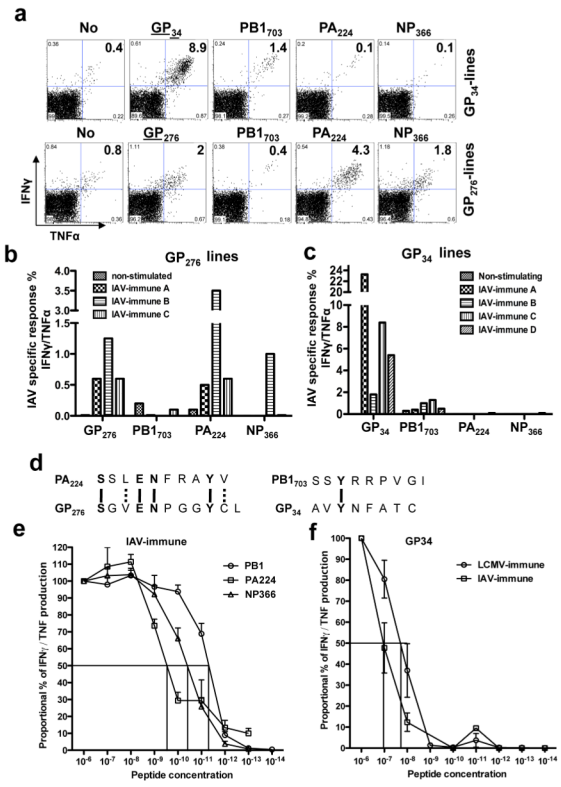

Figure 3. Screening for crossreactive-epitopes between LCMV and IAV

Splenocytes from 3 to 4 different IAV-immune mice (A-D) were cultured with LCMV-specific peptides GP33/34 (**a,c,f**) or GP_{276} (**a,b**) or IAV-specific peptides PA_{224}, $PB1_{703}$, or NP_{366} (**e**) for at least 3 wks. (**a,b,c**) LCMV-specific responses were tested by IFN**γ**/TNF production with GP33/34 or GP_{276}. Crossreactivity with IAV peptides was tested by ICS with $PB1_{703}$, PA_{224} or NP_{366}. As negative controls, 3 lines cultured in the presence of the RMA antigen presenting cells without any peptide produced no cytokines when stimulated by the different IAV- or LCMV-specific peptides. Also, 3 lines generated from naïve splenocytes produced no cytokines when stimulated by the different IAV- or LCMV-specific peptides shown here. (**d**) The sequence of either IAV PA_{224} and LCMV GP_{276} or IAV $PB1_{703}$ and GP_{34} were compared. Dashed lines indicate aa with similar properties between epitopes. The indicated concentrations of IAV-$PB1_{703}$, IAV-PA_{224} and IAV-NP_{366}, peptides **(e)** or LCMV-$GP_{33/34}$ peptides **(f)** were used in a 4 h ICS assay to stimulate the production of IFN**γ**/TNF by IAV-specific T-cell lines from 2-6 different IAV-immune mice or LCMV-specific T-cell lines from 2 LCMV-immune or 3 IAV-immune mice, respectively. The percentage of maximum cytokine response and the EC:50 are shown. IAV-specific lines from IAV-immune mice **(e)** showed high affinity for their respective cognate ligands, with $PB1_{703}$ showing the highest (EC:50 2×10^{-11}M), then NP_{366} (EC:50 2×10^{-10}M), followed by PA_{224} (EC:50 2×10^{-9}M). LCMV-$GP_{33/34}$ lines from LCMV-immune mice were 3-4 $\log_{10}$ lower affinity (EC:50 10^{-8}M) for $GP_{33/34}$ (**f**) than the cognate IAV peptides. However, the crossreactive $GP_{33/34}$-specific cells grown from IAV-immune splenocytes were a $\log_{10}$ lower in affinity to GP33/34 (EC:50 10^{-7}M) as compared to those grown from LCMV-immune splenocytes (**3f**).

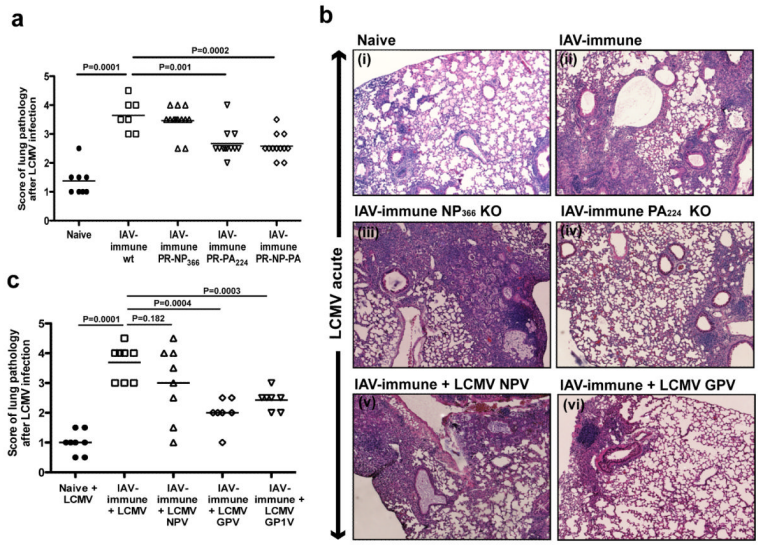

Figure 4. Decrease in lung pathology upon elimination of crossreactive T-cells by using LCMV and IAV epitope KO viruses

The lung pathology day 7 p.i. with LCMV was scored. Photographs depict a representative section showing a high power view of a small portion of one of the 4-5 different lung sections that were used for scoring in each individual mouse demonstrating the type of lung pathology observed in each group. (**a,b**) Mice were immunized with IAV, PR WT strain (□), or with IAV KO viruses PR-NP_{366} (▵), PR-PA_{224} (▿) or PR-PA-NP (◇), and challenged with LCMV. (**b,c**) Naïve (●) or IAV-immune mice (□) were infected with the WT LCMV or with different strains of LCMV knock down for NP_{396} (NPV) (▵) or GP33/34 (GP1V) (▿) or both GP33/34 and GP_{276} (GPV) (◇). Data were pooled from 3 experiments (n=2-5 mice/gp/expt).

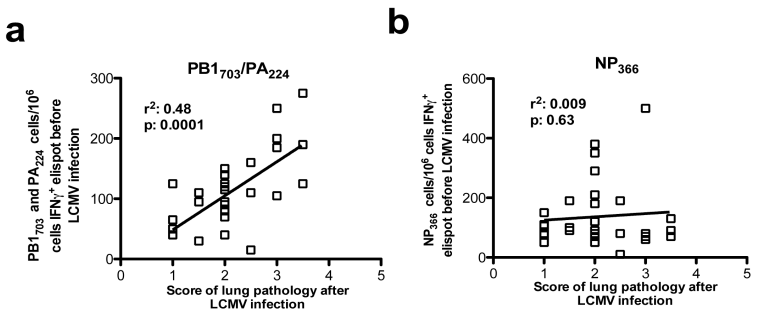

Figure 5. Severe lung pathology can be predicted

(a,b) IAV-specific memory cell hierarchies were tested by elispot assay of PBMC on each mouse, 6 wks after immunization. Mice were then challenged with LCMV and lungs were scored at day 7. The relationship between the intensity of lung pathology and the numbers of IAV-specific memory T-cells was evaluated by linear regression. Data was pooled from 3 experiments (n=5-10 mice/gp/expt).

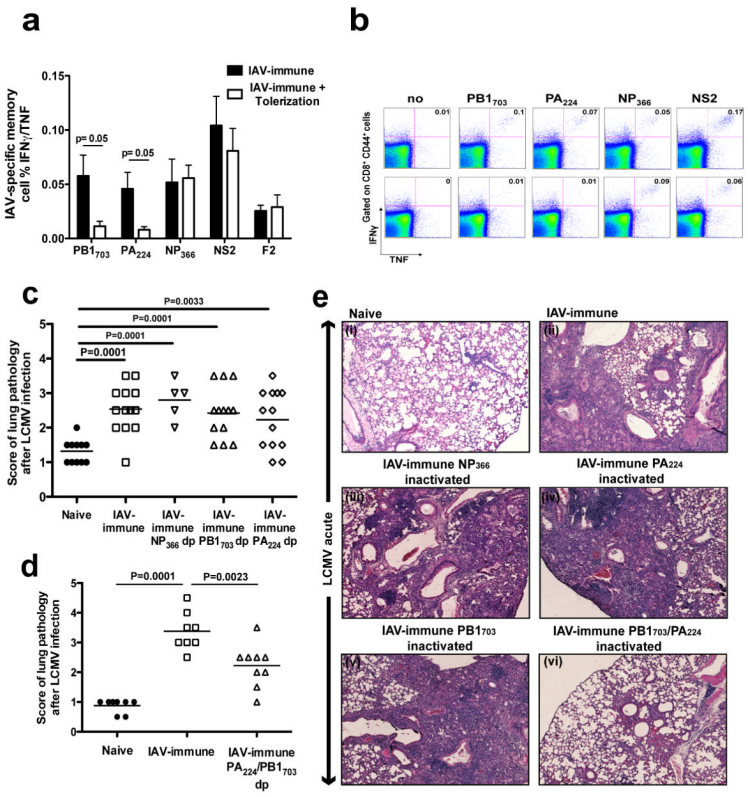

Figure 6. Severe lung pathology can be inhibited by tolerizing crossreactive IAV-specific CD8 T-cells

(a,b) 3 wks after IAV infection mice were either injected *i.v.* with PBS or with 250μg of IAV-specific peptides. 3 wks after treatment with IAV $PB1_{703}$, and PA_{224} IAV-specific CD8 memory splenic T-cell responses were tested by ICS for the production of IFNγ/TNF. Data are representative of 2 experiments and expressed as means plus or minus SEM (n=3-4/gp). Top and bottom rows in (b) are representative examples of ICS staining before and after peptide tolerization, respectively, with $PB1_{703}$, and PA_{224} peptides. **(c-e)** 3 wks after IAV infection mice were injected *i.v.* with 250 μg $PB1_{703}$, PA_{224} or NP_{366} peptides alone **(c,e)**, or with a mixture of $PB1_{703}$ and PA_{224} peptides **(d,e)**. The lung pathology was scored day 7 p.i. with LCMV. Photographs depict a representative section showing a high power view of a small portion of one of the 4-5 different lung sections that were used for scoring in each individual mouse demonstrating the type of lung pathology observed in each group. Data was pooled from 2-3 experiments (n=3-5 mice/gp/expt).

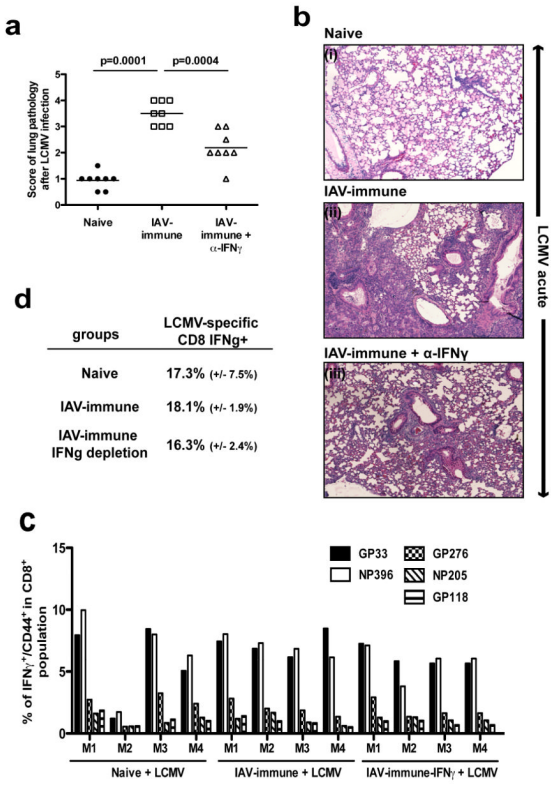

Figure 7. Lung pathology prevented by blocking IFNγ activity

(**a,b**) IAV-immune mice were either treated with anti-IFNγ (▵) or with PBS (□) *i.v.* day 0 and 3 and daily *i.p.* after LCMV infection. Lung pathology was scored. Photographs of representative examples of lung histology from each group are shown. Data were pooled from 2 experiments (n=3-4 mice/gp/expt). (**c,d**) Splenocytes were harvested at day 7 after LCMV infection from naïve, IAV-immune (non-depleted) or IAV-immune mice following depletion of IFNγ. LCMV-specific immune responses were characterized by surface staining of CD8, CD44 and in ICS assays examining peptides-specific IFNγ and TNF production.